FERMILAB-Conf-99/244-A

Cosmological Parameters and Power Spectrum from Peculiar Velocities

I. Zehavi

NASA/Fermilab Astrophysics Group, Fermi National Accelerator Laboratory, Box 500, Batavia, IL 60510-0500, USA

A. Dekel

Racah Institute of Physics, The Hebrew University, Jerusalem 91904, Israel

Abstract. The power spectrum of mass density fluctuations is evaluated from the Mark III and the SFI catalogs of peculiar velocities by a maximum likelihood analysis, using parametric models for the power spectrum and for the errors. The applications to the two different data sets, using generalized CDM models with and without COBE normalization, give consistent results. The general result is a relatively high amplitude of the power spectrum, with $\sigma_8 {\Omega_m}^{0.6} = 0.8 \pm 0.2$ at 90% confidence. Casting the results in the $\Omega_m - \Omega_\Lambda$ plane, yields complementary constraints to those of the high-redshift supernovae, together favoring a nearly flat, unbound and accelerating universe with comparable contributions from Ω_m and Ω_Λ. Further implications on the cosmological parameters, arising from a joint analysis of the velocities together with small-scale CMB anisotropies and the high-redshift supernovae, are also briefly described.

1. Introduction

In the standard picture of cosmology, structure evolved from small density fluctuations that grew by gravitational instability. These initial fluctuations are assumed to have a Gaussian distribution characterized by the power spectrum (PS). On large scales, the fluctuations are linear even at late times and still governed by the initial PS. The PS is thus a useful statistic for large-scale structure, providing constraints on cosmology and theories of structure formation. It is advantageous to estimate it from velocities, as these are directly related to the *mass* density fluctuations, and are effected by large scales and thus are approximately still linear.

In this work, we develop and apply a likelihood analysis for estimating the mass PS from peculiar velocities. This method uses the "raw" peculiar velocities without additional processing, and thus utilizes much of the information content of the data. It also takes into account properly the measurement errors and the finite discrete sampling. The simplifying assumptions made are that

the velocities follow a Gaussian distribution and that their correlations can be derived from the density PS using linear theory.

We use the two comprehensive available peculiar velocity data sets, the Mark III catalog (Willick et al. 1997) and the SFI catalog (Haynes et al. 1999a,b; Giovanelli, these proceedings). Mark III samples ~ 3000 galaxies within a distance of $\sim 70h^{-1}$Mpc around us, and SFI consists of ~ 1300 spiral galaxies with a more uniform spatial coverage in a similar volume. The typical relative distance errors of individual galaxies are $15-20\%$, and both catalogs are carefully corrected for systematic errors. It is interesting to compare the results of the two catalogs, especially in view of apparent discrepancies in the appearance of the velocity fields (e.g., da Costa et al. 1996, 1998). We explore the cosmological implications of the velocities on their own and in conjunction with constraints derived from other types of data.

2. Method

Given a data set $\mathbf{d}$, the goal is to estimate the most likely model $\mathbf{m}$. Invoking a Bayesian approach (and assuming a uniform prior), this can be turned to maximizing the likelihood function $\mathcal{L} \equiv \mathcal{P}(\mathbf{d}|\mathbf{m})$, the probability of the data given the model, as a function of the model parameters. Under the assumption that both the underlying velocities and the observational errors are Gaussian random fields, the likelihood function can be written as $\mathcal{L} = [(2\pi)^N \det(R)]^{-1/2} \exp\left(-\frac{1}{2}\sum_{i,j}^{N} d_i R_{ij}^{-1} d_j\right)$, where $\{d_i\}_{i=1}^{N}$ is the set of observed peculiar velocities and R is their correlation matrix. R involves the theoretical correlation, calculated in linear theory for each assumed cosmological model, and the estimated covariance of the errors.

The likelihood analysis is performed by choosing some parametric functional form for the PS. Going over the parameter space and calculating the likelihoods for the different models, one finds the PS parameters for which the maximum likelihood is obtained. Note that this method, based on velocities, in fact measures $P(k){\Omega_m}^{1.2}$ and not the PS by itself. Confidence levels are estimated by approximating $-2\ln\mathcal{L}$ as a χ^2 distribution with respect to the model parameters. We have extensively tested the reliability of the method on realistic mock catalogs, designed to mimic in detail the real data.

Our main analysis is done with a suite of generalized CDM models, normalized by the COBE 4-year data. These include open models, flat models with a cosmological constant and tilted models with and without a tensor component, where the free parameters are the mass-density parameter Ω_m, the Hubble parameter h and the power index n. We also use CDM-like models where the amplitude was allowed to vary.

A common problem in PS estimations is that the recovered PS is sensitive to the assumed observational errors, that contribute as well to the correlation matrix R. To alleviate this problem, we extend the method so that also the magnitude of these errors is determined by the likelihood analysis. This is done by adding free parameters that govern global changes of the assumed errors, in addition to modeling the PS, and provides a consistency check of the magnitude of the errors. We find, for both catalogs, a good agreement with the original error estimates, which allows for a more reliable recovery of the PS.

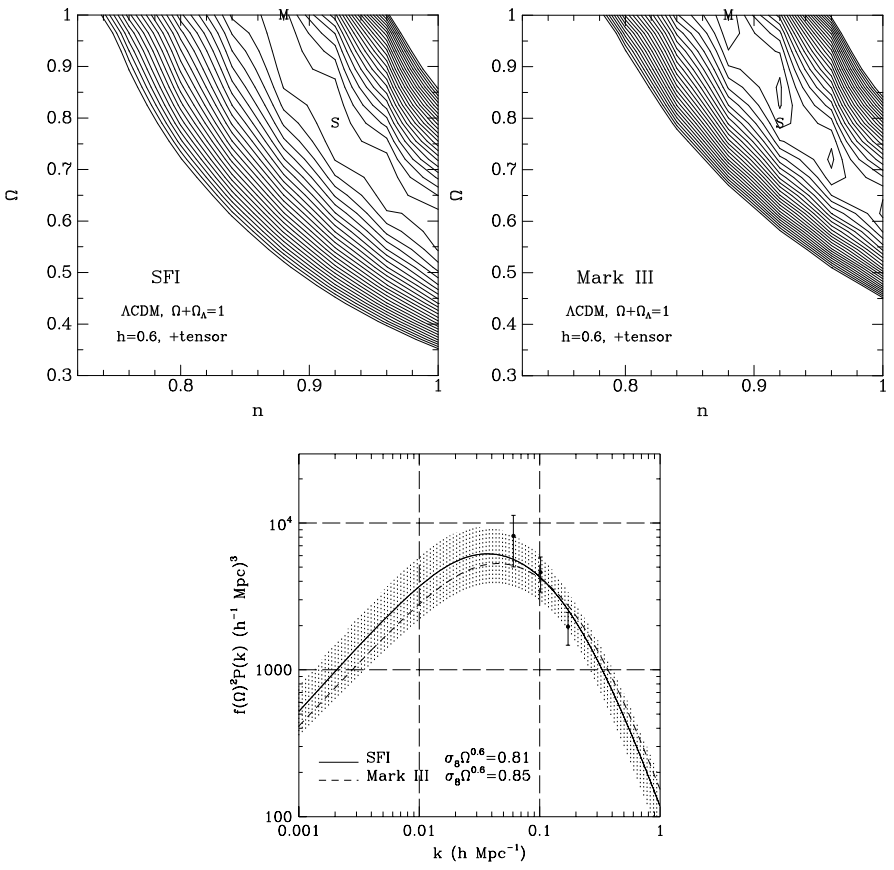

Figure 1. Likelihood analysis results for the COBE-normalized flat ΛCDM model with $h = 0.6$. Shown are $\ln\mathcal{L}$ contours in the $\Omega_m - n$ plane for SFI (top left panel; cf. Freudling et al. 1999) and for Mark III (top right; cf. Zaroubi et al. 1997). The best-fit parameters for SFI and Mark III are marked on both by 'S' and 'M', respectively. The lower panel shows the corresponding maximum-likelihood PS for SFI (solid line) and for Mark III (dashed). The shaded region is the SFI 90% confidence region. The three solid dots mark the PS calculated from Mark III by Kolatt and Dekel (1997), together with their quoted 1σ error-bar. (in the plot $\Omega \equiv \Omega_m$)

3. Results

Figure 1 shows, as a representative example, the results for the COBE-normalized flat ΛCDM family of models, with a tensor component in the initial fluctuations, when setting $h = 0.6$ and varying Ω_m and n. Shown are $\ln\mathcal{L}$ contours for the SFI catalog and for Mark III. As can be seen from the elongated contours, what is determined well is not a specific point but a high likelihood ridge, constraining a degenerate combination of the parameters roughly of the form $\Omega_m\, n^{3.7} = 0.6 \pm 0.1$, in this case. The corresponding best-fit PS for the two catalogs is presented as well, with the shaded region illustrating the 90% confidence region obtained from the SFI high-likelihood ridge.

These results are typical for all other PS models we tried. For each catalog, the different models (including the ones with free normalization) yield similar best-fit PS, falling well within each others formal uncertainties and agreeing especially well on intermediate scales ($k \sim 0.1\, h\,\mathrm{Mpc}^{-1}$). The similarity of the PS obtained from SFI with that of Mark III, which is apparent in the figure, is also illustrative of the other models. This indicates that the peculiar velocities of the two catalogs, with their respective error estimates, are consistent with arising from the same underlying mass density PS. This does not preclude possible differences that are not picked up by this statistic, but can be viewed as another indication of the robustness of the results. Note also the agreement with an independent measure of the PS from the Mark III catalog, using the smoothed density field recovered by POTENT (the three dots; Kolatt & Dekel 1997).

More details on the method and results can be found in Zaroubi et al. (1997) and Freudling et al. (1999), regarding the applications to Mark III and to SFI, respectively. The robust result, for both catalogs and all models, is a relatively high PS, with e.g. $P(k = 0.1\, h\,\mathrm{Mpc}^{-1}){\Omega_m}^{1.2} = (4.5 \pm 2.0) \times 10^3\, (h^{-1}\mathrm{Mpc})^3$. An extrapolation to smaller scales using the different CDM models gives ${\sigma_8\Omega_m}^{0.6} = 0.8 \pm 0.2$. The high-likelihood ridge is a feature of all COBE-normalized CDM models, corresponding to a general constraints on the combination of cosmological parameters of the sort $\Omega_m\, {h_{60}}^{\mu}\, n^{\nu} = 0.6 \pm 0.2$, where $\mu = 1.3$ and $\nu = 3.7,\ 2.0$ for flat ΛCDM models with and without tensor fluctuations respectively. For open CDM, without tensor fluctuations, the powers are $\mu = 0.9$ and $\nu = 1.4$. These error-bars are crude, reflecting the 90% formal likelihood uncertainty for each model, and the variance among different models and catalogs. Note that our results are suggestive of somewhat higher values of ${\sigma_8\Omega_m}^{0.6}$ and Ω_m than those implied by some other methods (such as from the clusters abundance and the different β measures).

4. $\Omega_m - \Omega_\Lambda$ Constraints

We have recently extended the analysis of COBE-normalized CDM models to models with general values of Ω_m and Ω_Λ (Zehavi & Dekel 1999). Although the Ω_Λ dependence comes in only indirectly through the COBE normalization, such results are particularly interesting as they can be combined with other constraints in the $\Omega_m - \Omega_\Lambda$ plane.

Figure 2 illustrates constraints in the $\Omega_m - \Omega_\Lambda$ plane, showing the confidence contours obtained by the Supernova Cosmology Project (Perlmutter et al. 1999;

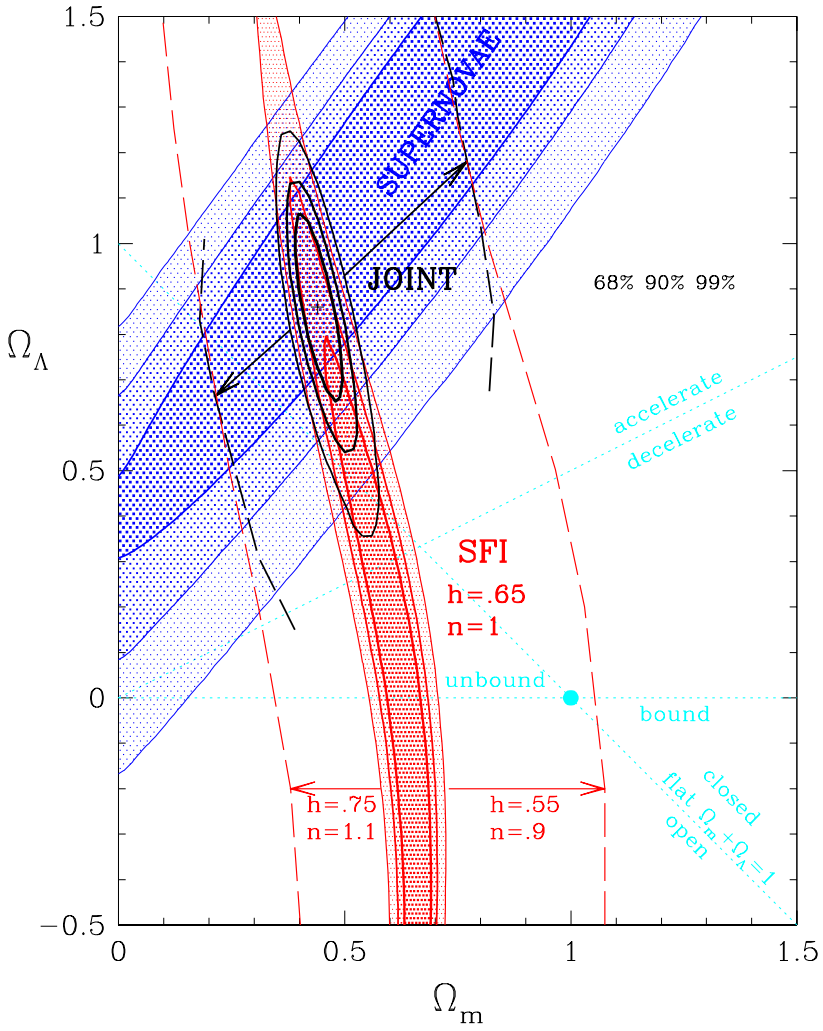

Figure 2. Constraints in the $\Omega_m - \Omega_\Lambda$ plane arising from the high-z SN (the blue inclined contours; Perlmutter et al. 1999) and from a likelihood analysis of the SFI peculiar velocities (the red roughly vertical contours). The 68, 90 and 99% confidence regions are shown for both. The peculiar velocity contours are for $n = 1$, $h = 0.65$, with the shifted red dashed lines showing the effect of changing the values of these parameters. The corresponding joint confidence regions of the velocities and the SN are shown as the black overlapping ellipses (Zehavi & Dekel 1999).

consistent with the findings of the High-z Supernova Search Team, Riess et al. 1998) as well as the contours from our SFI likelihood analysis, performed for fixed values of $n = 1$ and $h = 0.65$. The velocity analysis constrains an elongated ridge in this plane of a nearly fixed Ω_m and varying Ω_Λ. The analogous constraints from the Mark III catalog are quite similar, except that the (fairly uncertain) upper bounds on Ω_Λ are slightly tighter. A change in the values of n and h essentially shifts the ridge toward a higher or lower Ω_m, for smaller and larger values of these parameters, respectively. (This is another manifestation of the degeneracy between these parameters mentioned earlier). Their acceptable range is therefore needed to be determined a-priori from other constraints. For a reasonable range of these parameters, the effect is denoted in the plot by the shifted dashed lines.

The corresponding joint contours of the velocities and the SN, obtained by multiplying the likelihoods, are also shown on the plot, and here as well one should consider the area bounded by the dashed lines. Taking into consideration concurrently these two independent sets of constraints thus implies a considerable contribution from both Ω_m and Ω_Λ. Specifically, models with small Ω_m and small Ω_Λ, that are still allowed by the SN constraints alone, are disfavored when the constraints from SNe and peculiar velocities are considered jointly; together, they make a stronger case for an unbound accelerating universe with a positive cosmological constant.

5. Further Analysis

We are currently in the final stages of performing a joint analysis of peculiar velocities together with constraints obtained from CMB anisotropies and from the high-z SN (Bridle et al. 1999). The distinct types of data complement one another, each constraining different combinations of the cosmological parameters, and together can potentially set tight constraints. Figure 3 illustrates the constraints obtained for each of these data sets in the $\sigma_8 - h - \Omega_m$ space, for the scale-invariant *flat* ΛCDM family of models. The results shown here are for the SFI catalog. Since the COBE constraint is now included in the CMB data, the velocity analysis is performed free of the COBE normalization. The high-z SN constraints appear here as bounds on Ω_m (as we assume flat ΛCDM). The value of h is left free to be determined by the likelihood analysis.

The figure demonstrates that these three data sets provide roughly orthogonal constraints, with a significant overlap beyond the 2σ level, that allows a meaningful joint parameter estimation. The best-fit values obtained from the joint analysis of the three data sets are $\Omega_m = 0.52$, $h = 0.57$ and $\sigma_8 = 1.1$ (corresponding to $\sigma_8 {\Omega_m}^{0.6} = 0.74$). The 95% confidence regions on the individual parameters, obtained by marginalizing over the other two parameters, are $0.27 < \Omega_m < 0.54$, $0.54 < h < 0.85$ and $1.02 < \sigma_8 < 1.67$. See also Lahav, these proceedings, for a presentation of the results in the $\sigma_8 {\Omega_m}^{0.6} - \Omega_m h$ plane.

Additional work in progress includes an application of the likelihood method to other peculiar-velocity data, such as velocities of galaxy clusters (e.g., the SMAC sample; Hudson et al. 1999, Smith, these proceedings) or the local SN velocities, both probing larger scales with relatively high accuracy per object. With regard to the cluster velocities, we are attempting to properly take into

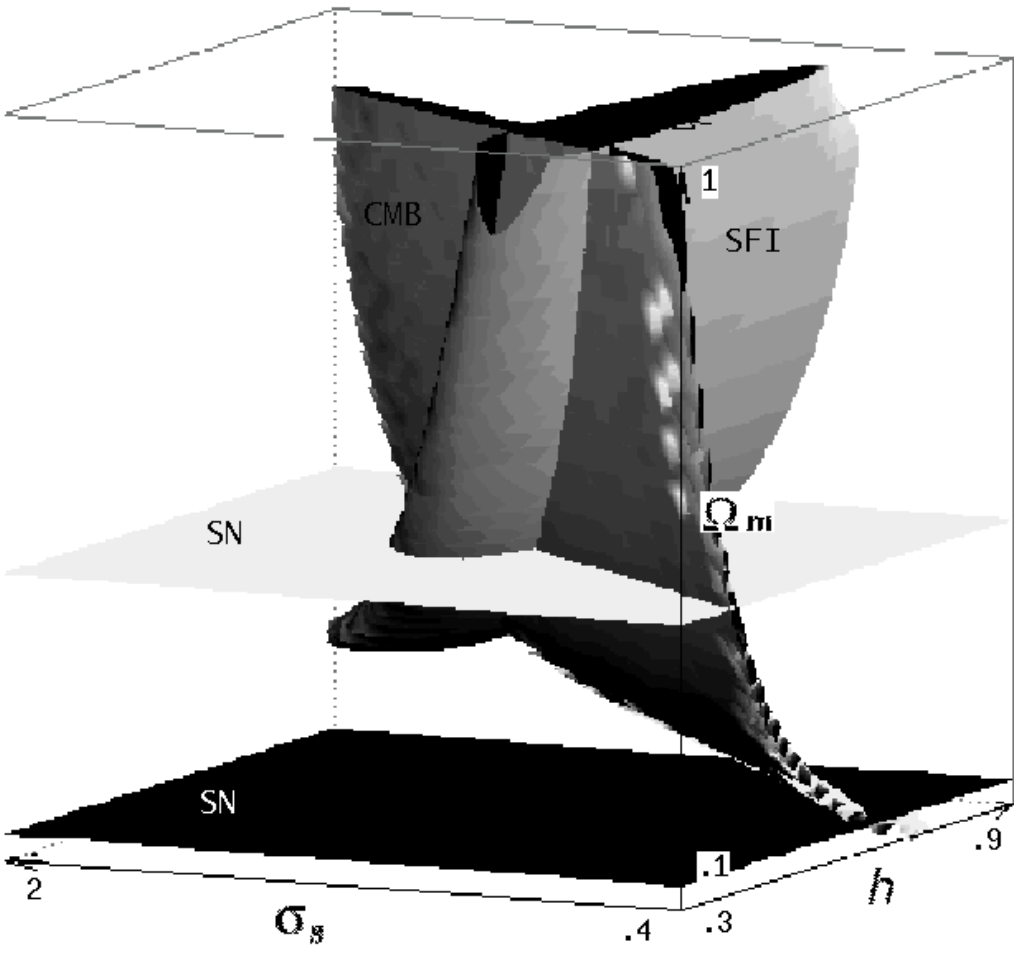

Figure 3. The 95% confidence regions obtained from the SFI velocities, the CMB anisotropies and the high-z SN, in the $\sigma_8 - h - \Omega_m$ space, for scale-invariant flat ΛCDM models (Bridle et al. 1999).

account in the analysis the fact that they are sampled at high density regions (Zehavi et al., in prep.).

Finally, another project underway is an attempt to obtain model-independent band-power estimates of the PS from peculiar velocities, using an iterative quadratic estimator scheme, which greatly improves the computational effort. (Such an approach is commonly applied to CMB measurements, e.g Bond, Jaffe, & Knox 1998). This allows to relax the a-priori assumption of the PS form, and would illuminate the actual constraints on the different scales and their cross-correlations (Zehavi & Knox 1999).

Acknowledgments. We thank our collaborators in different aspects of the work presented here: S. Bridle, L.N. da Costa, A. Eldar, W. Freudling, R. Giovanelli, M.P. Haynes, Y. Hoffman, T. Kolatt, O. Lahav, J.J. Salzer, G. Wegner and S. Zaroubi. This research was supported by US-Israel Binational Science Foundation grant 95-00330 and Israel Science Foundation grant 546/98 at HU, and by the DOE and the NASA grant NAG 5-7092 at Fermilab.

References

Bond, J. R., Jaffe, A. H., & Knox, L. 1998, Phys.Rev.D, 57, 2117

Bridle, S. L., Zehavi, I., Dekel, A., Lahav, O., Hobson, M. P., & Lasenby, A. N. 1999, in preparation

da Costa, L. N., Freudling, W., Wegner, G., Giovanelli, R., Haynes, M. P., & Salzer, J. J. 1996, ApJ, 468, L5

da Costa, L. N., Nusser, A., Freudling, W., Giovanelli, R., Haynes, M. P., Salzer, J. J., & Wegner, G. 1998, MNRAS, 299, 425

Freudling, W., Zehavi, I., da Costa, L. N., Dekel, A., Eldar, A., Giovanelli, R., Haynes, M. P., Salzer, J. J., Wegner, G., & Zaroubi, S. 1999, ApJ, 523, 1

Haynes, M. P., Giovanelli, R., Salzer, J. J., Wegner, G., Freudling, W., da Costa, L. N., Herter, T., & Vogt N. P. 1999a, AJ, 117, 1668

Haynes, M. P., Giovanelli, R., Chamaraux, P., da Costa, L. N., Freudling, W., Salzer, J. J., & Wegner, G. 1999b, AJ, 117, 2039

Hudson, M. J., Smith, R. J., Lucey, J. R., Schlegel, D. J., & Davis, R. L. 1999, ApJ, 512, L79

Kolatt, T., & Dekel, A. 1997, ApJ, 479, 592

Perlmutter, S. et al. 1999, ApJ, 517, 565

Riess, A.G. et al. 1998, AJ, 116, 1009

Willick, J. A., Courteau, S., Faber, S. M., Burstein, D., Dekel, A., & Strauss, M. A. 1997, ApJS, 109, 333

Zaroubi, S., Zehavi, I., Dekel, A., Hoffman, Y., & Kolatt, T. 1997, ApJ, 486, 21

Zehavi, I., & Dekel, A. 1999, Nature, 401, 252

Zehavi, I., & Knox, L. 1999, in preparation